Study of the Helicon Source Operation in the Variable Specific Impulse Magnetoplasma Rocket (VASIMR) Experiment

- Final Technical Report -

Principal Investigator: Prof. Kim Molvig

Co-PI: Dr. Oleg Batishchev

Period: July 1, 2002 – February 28, 2003

Address: Massachusetts Institute of Technology
NW16-243, 77 Massachusetts Ave, MA 02139

NASA Grant: NAG9-1455

Summary

During research period the following models of the VASIMR helicon discharge have been further developed and applied to analyze the on-going VX-10 ASPL experiment:

A) 1D semi-analytical model for a mixed-collisional propellant flow
B) 0D power and balance model for the whole helicon discharge

In this particular research period we have concentrated on the MW-level performance of the VASIMR helicon source. Favorable high-power scaling and reduced ionization costs were obtained, and presented at the VASIMR NASA review in the Fall '02. This Grant is continuation of the previous NAG9-1224 award. The research results are summarized in 14 publications; they were presented as 20+ talks at the major International Conferences and scientific seminars at the leading Academic and Research Institutions. The reported results allowed helicon discharge characterization, understanding of the several experimental observations, and helped to make predictions and propose structural modifications for the advanced VASIMR helicon source operation.

Motivation

The integral performance of the high, variable specific impulse I_{sp} thruster being developed under the VASIMIR project [1] by ASPL/NASA depends on the efficiency of the helicon plasma source. Current ASPL experimental data shows stable helicon source [1-2] performance for various gases. However, there is new evidence that current models and theories of the helicon discharge are incomplete. For instance, RF-power absorption may have several resonances; performance with mixtures of gases is different from pure hydrogen or helium; retarded probe analyzers show a large population of energetic ions with non-Maxwelian distribution; neutral pressure jumps by a factor of 4 during discharge; heat deposition onto inner wall has a non-monotonic spatial profile. There is an indication that a fraction of RF-power goes into ions, and that charge-exchange collision process and residual vacuum tank pressure influence the dynamics of the helicon discharge. Because experimental diagnostics are limited new theoretical-numerical models are required to understand VX experiment helicon operation.

The need for the development of various models comes from the analysis of the typical VASIMR discharge conditions, listed below

Parameters of the VASIMR plasma

Dimensions of the VX-10 helicon source are about 10x100 cm [2];
Magnetic field is non-uniform, varies in the 10-600 Gs range;
Neutral gas pressure varies in the 1-600 mTorr range;
Neutral gas density alters from $5x10^{15}$ cm^{-3} to $1x10^{13}$ cm^{-3};
Plasma density is about $1\text{-}2x10^{12}$ cm^{-3}
Electron temperature is about 5-10 eV;
Ion exhaust velocity is about 40 km/sec, corresponding to flow energy ~16eV;
Plasma flow is sub-sonic or super-sonic;
Heating power is in 3 KW-10KW range (and up to MW-level);
RF frequency is 13.6 MHz (and up);
Mass flow rate is 10-1000 sccm.

Introduction

VASIMR is a unique electrode-free electric propulsion system [1-4], which has a potential of achieving specific impulse on the order of 30Ksec with 50% energy efficiency. Fuel efficiency depends entirely on that of a plasma source. Presently the VASIMR project considers the helicon discharge plasma source [5,8] a primary candidate.

A typical VASIMR thruster combines three distinct areas i) plasma source, ii) plasma RF-heating cell and iii) magnetic nozzle, as shown in the Fig.1. The most probable propellant is H_2 to achieve maximum specific impulse I_{sp} at a given mass fueling rate. There are several important collisional processes taking place in such a thruster. Firstly, there are a few inelastic channels to break incoming molecular gas into neutral atoms, ionization and excitations of neutrals, and wall interactions [6-7].

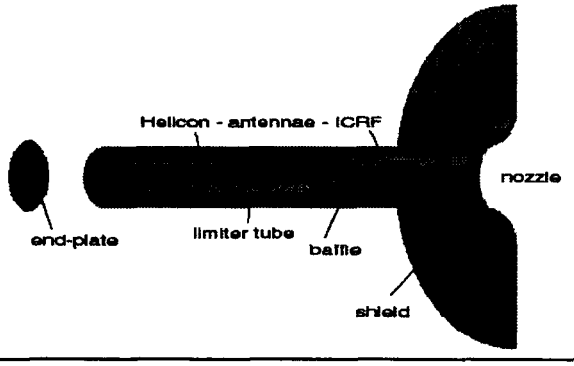

Figure 1 – Plasma facing part of a typical VASIMR engine

Next, there are a number of elastic collisions of potential importance: Coulomb interaction, resonance charge-exchange, etc [9-10]. The typical Knudsen number for the different elementary processes varies in a 0.1-10 range, which indicates that the short mean free path limit [6] fails, and a pure kinetic analysis is required [11-12]. There are a few approaches to that.

Comparison of particle-in-cell and finite difference methods shows that the Fokker-Planck approach is computationally more efficient [22]. Particle methods suffer from the intrinsic statistical noise, which occurs because of the limited number of model particles per cell, and it is always 6-8 orders of magnitude larger than the "natural physical" noise. Finite-difference methods are free of the statistical fluctuations in the first place, and allow studying both coarse and fine effects. From the mathematical point of view numerical particle solution is always non-converged (oscillations recede as an inverse square root of the number of trajectories), while grid methods may give a converged solution up to the computer accuracy $\sim 10^{-14}$.
Next, finite numbers of particles per cell in the numerical simulation make it impossible to resolve accurately enough an important energetic tail of the electron and ion distribution functions, because the tail is normally exponential function of energy. Practical limit of the resolution (for 10-100K particles per cell) is 3-4 thermal velocities. Time averaging helps for steady-state regimes only. Thus, non-linear time-dependent study of the transient regimes is impossible in principle.
Grid method with a non-uniform mesh in the velocity space allows equally accurate resolution of the cold core and very energetic tail (100 thermal velocities) of the distribution function. These

tails are important for plasma diagnostics with probes and neutral beams; they also determine plasma thermal conductivity.

Lastly, in the regimes of interest, regions of sharp spatial gradients of plasma parameters are expected. The universal tool to study such fronts is provided by adaptive grids in space [23].
While the pure kinetic approach is an ultimate goal, we are also developing simplified 0-D plasma chemistry model, which allows us to obtain crucial parameters of the helicon discharge: plasma and neutral species composition, temperatures of all plasma components, energy/particle fluxes out of the plasma source and heat fluxes onto wall. This model is a continuous development of our original model [16]. The latest additions include possibility of Lyman-α radiation reflection and recapture, as well as it artificial reduction to study the energy efficiency of the VASIMR thruster.
This simple 0-D model uses critical information about propellant flow in the system of pipes as given by our 1-D semi-analytical hybrid model, which was also developed under this award. New fully kinetic 2V2D BGK-type model for a rarified gas flow independently verifies its results in a system of connected channels. Information about plasma flow is taken from our fully kinetic Fokker-Planck model that was described in the early publications [16-17]. These results are compared to recent RPA data [21] for the ion distribution function obtained for the VX-10 experimental setup.

All these numerical models have been applied to:
a) understand operation of the helicon plasma source in the VASIMR VX-3 and VX-10 experiments;
b) make predictions for the future space VF-10/25 thruster [4,5], and
c) propose practically feasible suggestions on how to boost fuel and energy efficiencies of the critical elements of the plasma thrusters, based on the VASIMR technology.

Current status of VX-10 [5] experiment shows about 40% fuel efficiency for hydrogen, deuterium and helium discharges when they operate in a high-density mode. It's not clear what determines transition to this important mode. We use a few numerical models to study operational regimes of the helicon plasma source.

Energy and particle balances are studied using 0-dimentional model of gas discharge [16]. The following processes are accounted for hydrogenic discharge: molecule and molecular ion dissociation, neutral ion ionization and excitation, charge-exchange, wall conversion, formation of heavy ions, etc. Model predicts plasma and gas species densities and temperatures to be very close to that measured in the experiment. The model is used to assess effects of gas baffles, vacuum tank, gas pre-heating, altering dimensions of the quartz tube, etc. on the hydrogen and helium discharges performance.

Finally we discuss fully kinetic 1D2V and Fokker-Planck-Boltzmann models of the gas [11,18,24] and plasma flows [12, 25-26]. They account for spatial variation of ambipolar potential and external magnetic field and basic elastic and inelastic collisions. Kinetic simulations show that the distribution functions of both gas and plasma species differ from the Maxwellian due to external heating, non-local transport and trapping in the magnetic field. IDF is in concert with recent RPA measurements [21]. Our numerical results indicate that specific impulse on the order of 3-4Ksec is achievable by the helicon source along, and 8-10Ksec with additional ICRF-heating of the ions for the 3-10kW input electrical power.

A) 1D semi-empirical model for propellant flow in pipes

Our initial numerical and theoretical studies [16-17] have indicated that the degree of gas ionization in the helicon source is low, on the order of 1%. This fact allows viewing propellant flow in the gas feeding - plasma source system ([19], shown in the Fig.2) as entirely independent of that of plasmas.

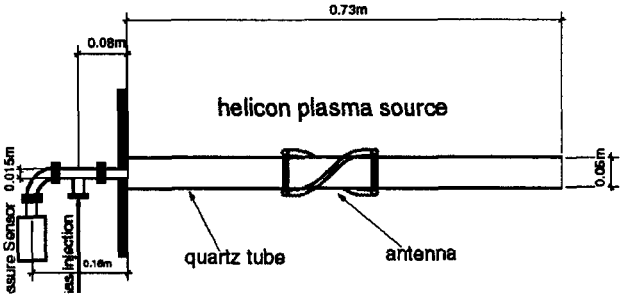

Figure 2 – Gas feed – quartz tube of VX-10 VASIMR configuration

Simple estimate show that gas flow in the system will be strictly laminar. Indeed, from the experimental measurements: pressure drops along the system from PI≈100mtorr in the gas inlet to PVC≈1mtorr in the vacuum chamber, and mass flow rate μ=80sccm we find that the characteristic Reynolds number of the flow

$$Re = V\,d / \nu \approx 20 << R_{cr} \approx 2300 \qquad (1)$$

is much smaller than the critical value [14], R_{cr}, which marks the onset of a turbulent regime.
On another hand simple consideration shows that the Knudsen number [13] of the propellant flow

$$Kn = 2\lambda/d \approx 0.5\text{-}2 \qquad (2)$$

Hence, we can view the gas flow to be a composition of the viscous and free molecular laminar flows (as shown in the Fig.3 below).

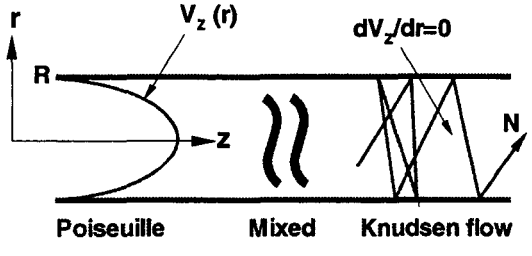

Figure 3 – Scheme of hybrid model

Hybrid Poisseuille - Knudsen model for mixed-collisional gas flow can be easily derived on the basis of two classical results. For the viscous flow one can apply Poisseuille result [14] for a pipe flow: mass throughput in a pipe is proportional to the pressure gradient and to 4-th power of the pipe's radius R:

$$\mu_P = A(T)\, R^4(z)\, dP/dz \qquad (3)$$

where parameter A(T) contains viscosity, etc.

For a similar free molecular flow one can use analogous result, obtained by Knudsen model [13]:

$$\mu_K = B(T)\, R^3(z)\, dP/dz \qquad (4)$$

Now, taking into account that mass throughput is constant along axial direction, and that asymptotic expressions (3)-(4) should be valid for the limits Kn→0 and Kn→∞, respectively, we may find the following hybrid expression:

$$\mu = \int \pi r^2 \rho\, V_z\, dr = const = \mu_P + (\mu_K - \mu_P)\,[\,1 - \exp\{-Kn\}\,] = C(T,P,z)\, dP/dz \qquad (5)$$

where C(T,P,z) is a new composite function. By inverting Eq. (5) we obtain the following finite-difference expression:

$$\Delta P = \mu / c(T,P,z)\, \Delta z \qquad (6),$$

which can be integrated numerically, say from the gas injector (P=PI) up to the end of the quartz tube of the helicon source. Results for He are shown in Fig.4.

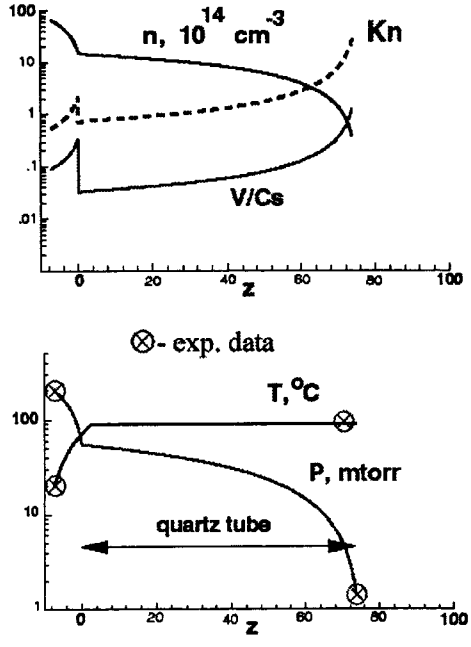

Fig.4. Hydrogen gas flow

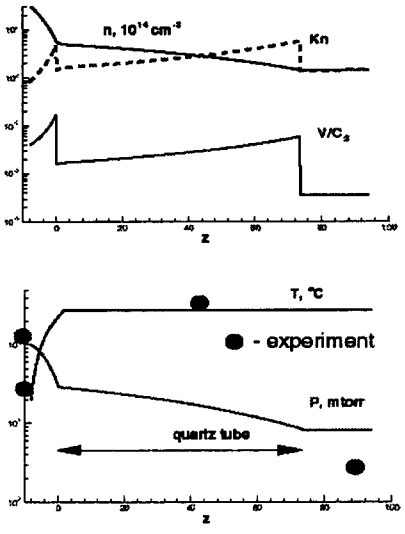

Figure 4 – Profiles of helium gas flow parameters for the VX-10 geometry

As one can see from the bottom chart in the Fig.4 agreement with experimental data for the pressure drop along the system are within 1% of accuracy for constant helium flow rate μ=200sccm. Note that axial temperature profile is a fit to the experimental measurements of the quartz tube temperature. We assume that as neutral gas has the same temperature profile due to energy exchange with the wall.

Interestingly enough 80% of the pressure drop occur in the short (8cm) and narrow (1.5cm in diameter), 20% in the quartz tube (Fig.2), and under 1% in the rest sections of the system (magnet bores, etc.). One can see that our original assumption about mixed viscous-free molecular flow is verified a posteriori (as de-facto Knudsen number, Kn, is in the 0.5-5 range).

The helium gas flow experiences transition viscous →molecular → viscous → molecular 3, and accelerates 2 times. What is the most important for our immediate goal is that mean gas flow is very subsonic with average Mach number <M> ≈0.03-0.05.

To crosscheck we benchmark hybrid model against experimental data for molecular hydrogen gas flow at μ=100sccm in the same VX-3 [16] configuration. Corresponding results are close to those in Fig.4.

The major results remain the same: gas flow is very viscous and subsonic, gas density in the center of the quartz tube (where helical antenna is located) is on the order of $N \approx 3\text{-}5 \times 10^{14} cm^{-3}$.

Comparison of old and new quartz tubes

Recent results from the VX-10 equipped with a longer quartz tube show two-fold increase of the plasma density in the discharge [19]. We apply 1D model to study gas flow in the original and new tubes. Their geometrical parameters are as follows. Old tube is 5cm in diameter and 70cm long. New tube is 1m long and has slightly larger diameter of 5.5cm.

Though, dimensions of the two tubes are different, surprisingly enough they have the same resistance to the hydrogen gas flow. As one can see from the Fig.5 both pressure and density drops along the tubes coincide with in a few percent. Also in the experiment the RF-antenna position was fixed at the same position closer to the left side of the tube, and the input power stayed the same at about 3 kW.

Thus, the only difference of the two discharges is in the gas density at the location of RF-energy deposition source. With the longer tube the neutral gas density gradient is shallower, energy is released to a more dense gas (and plasma too). Because gas density is higher, we can guess that the ionization may be more efficient, and the discharge will yield more plasma for the equivalent amount of energy transmitted into the electron species.

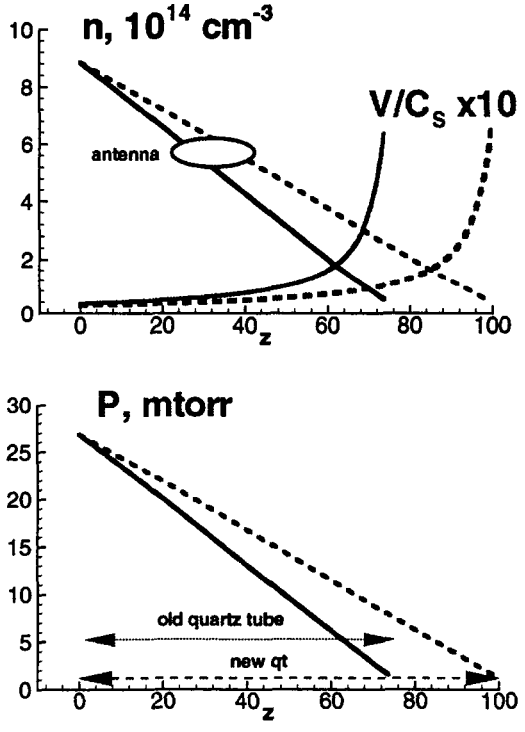

Figure 5 - gas profiles in old and new quartz

Use of conical tubes instead of cylindrical

If these arguments are correct, we can try finding simple ways to keep neutral gas density higher in the quartz tube volume. One of the possibilities to keep gas density flatter as it accelerates axially – is to use a quartz tube of varying cross-section. Because the helicon RF-antenna has fixed dimensions we propose using conical shape quartz tubes with average radii approximately equal to that of the internal RF-antenna radius. In this case two-way use of the new tubes becomes possible automatically.

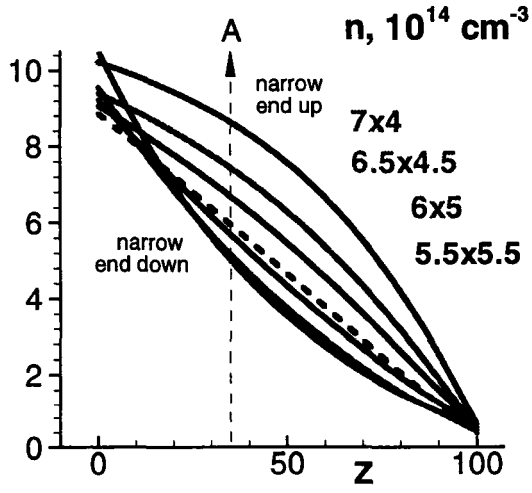

Figure 6 - gas density in conic tubes

In Fig.6 we present calculated gas density profiles for a set of three tubes with the same length of 1m and the same mean internal radius of 5.5cm. Their small-large radii are as follows: 6x5cm, 6.5x4.5cm and 7x4cm. For comparison we present data for a straight pipe (single linear curve in Fig.6). Each pair of curves – one is folded in and another out – correspond to the same conic-shape tube oriented in two different ways (gas expansion or compression). As one can see simple change of the tube axial orientation allows nearly 100% variation of the gas density in the middle of the pipe. On another hand, when the tube's cross-section is reducing along the flow direction, gas density has much more flat profile. In this case we may expect more efficient gas ionization by electron impact, and higher overall fuel efficiency of the VASIMR thruster. Note that if we'll take into account gas loss due to ionization, the reduction of tube radius has to be large to compensate it. Shaping of the external magnetic field will be obviously required (magnetic choke) to avoid hot magnetized plasma striking the internal surface of the tube, causing energy loses and unwanted damage.

B) Mass and energy balance model for VASIMR plasma source

The helicon has proven to be a robust and efficient plasma source [8]. The helicon source consists of a dielectric (quartz) tube embraced by the helicon antenna, which launches electromagnetic waves in the plasma. Electrons are heated through possibly collisional or Landau damping of the waves in the plasma. This process is not included self-consistently here; it is a subject of a separate study. In this model we assume that a certain power, W, is transmitted to the electrons. The electron temperature and density in the source are 6eV and $2x10^{12}$ cm^{-3}, respectively, as measured in the ASPL experiments [5, 19].

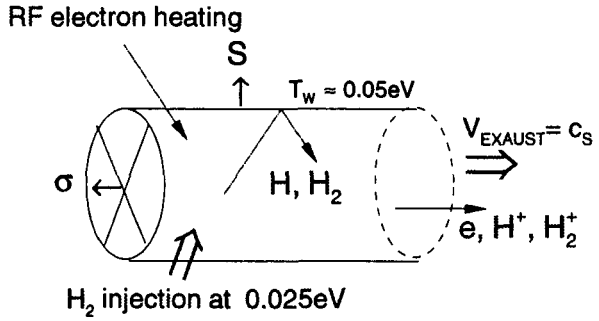

Figure 16 – Model of a helicon discharge

Let's accept the following physical model of a helicon plasma source, as shown in Fig.16. Next, we consider the accepted models for the main physical processes taking place in the discharge.

Electron and ion transport. The electrons are magnetized by a relatively strong magnetic field of 0.1-0.6T. The electron gyroradius is about 10-2cm, ion gyroradius – 0.2cm, which is much smaller than 10cm - tube's diameter. The gyroradius becomes huge in the nozzle. Cross-field transport is weak because of the low plasma density. The plasma flux onto outer wall is negligible. Electrons strictly follow field lines, which are parallel to the cylinder axis. At one of the tube's ends there is a floating potential wall. The floating potential value for hydrogen (deuterium) plasma is 2.8(3) Te. Thus, the majority of the electrons are reflected back. There is a small residual particle/energy flux onto the end plate. We anticipate that the continuous puffing of H_2 through the inlet will keep the plasma density low near the end plate. Therefore, we neglect the heat and mass flow onto the floating end plate. At the open end of the quartz tube the plasma is leaving the system at a fraction of sound speed.

Plasma exhaust velocity. The Debye length of the plasma in typical Helicon hydrogen discharge, λ_D, is on the order of 10^{-3} cm, while the tube dimension is on the order of 1m. Therefore, plasma in the volume is quasineutral and the plasma flow is ambipolar. We assume that the ion's exhaust velocity is sub-sonic with a fraction of the ion sound speed, $C_{Si}=(2T_e/M_i)^{0.5}$. The electron density is equal to the combined density of all ion species (H^+, H_2^+, H_3^+ here). The electron exhaust velocity is such to automatically maintain the ambipolarity of plasma $V_e=(n_{H+}C_{SH+} + n_{H2+}C_{SH2+} + n_{H3+}C_{SH3+})/ (n_{H+} + n_{H2+} + n_{H3+})$. Neutral exhaust velocity is assumed to be sub-sonic as well with $C_{SN}\approx 0.03\ (2T_N/M_N)^{0.5}$. Because the neutral temperature is significantly lower than the electron temperature, ions exhaust the helicon source at a much higher pace than the cold neutrals.

Energy exhaust and wall fluxes. Sonic neutral exhaust carries along energy flux:

$$Q^E = \sigma j^E (CkT + \frac{1}{2} M C_s^{\ 2}) = \sigma (C+1)\, nkT\ V_T \qquad (7)$$

where σ is a quartz tube cross-section, VT is thermal velocity, C is specific heat. Wall neutral flux requires separate attention. We assume that gas (and plasma) has Maxwellian distribution:

$$f_M(n,T) = \frac{n}{(\pi^{1/2} V_T)^3} \cdot \exp\left\{-\frac{v^2}{V_T^2}\right\} \qquad (8)$$

and fills the tube homogeneously. We may easily find the kinetic energy and particle fluxes onto wall to be:

$$q^W(n,T) = \int_{-\infty}^{+\infty}\int_{-\infty}^{+\infty}\int_{0}^{+\infty} v_x \frac{Mv^2}{2} f_M dv_x dv_y dv_z =$$
$$\frac{nMV_T^3}{\pi^{3/2}} \int_0^{+\infty}\int_0^{+\infty} x \frac{x^2+p^2}{2} 2\pi p \cdot e^{-x^2-p^2} dx dp = \qquad (9)$$
$$\frac{nMV_T^3}{\pi^{1/2}} 2 \int_0^{+\infty}\int_0^{+\infty} \frac{1}{4} r e^{-r-s} dr ds = \frac{nkTV_T}{\pi^{1/2}}$$

and, respectively,

$$j^W(n,T) = \int_{-\infty}^{+\infty}\int_{-\infty}^{+\infty}\int_{0}^{+\infty} v_x f_M dv_x dv_y dv_z = \frac{1}{4} n V_T \qquad (10)$$

Note that this is just kinetic energy flux. Non-mono-atomic neutrals bringing also rotational energy to the wall. The expression for total energy deposited is

$$Q^W = (S+\sigma)(\alpha + \frac{C-1.5}{4}) \cdot nkTV_T \qquad (11)$$

where $\alpha=\pi^{-0.5}$. All particles that collide with wall are coming back with wall temperature $T_W \approx 500^oC$.

Temporal evolution of the density and temperature of the 6 plasma species: {*e*, H_2, H, H^+, H_2^+, H_3^+} is determined by cold gas puff rate, electron heating rate, energy exchange with wall, mass/energy exhaust and various inelastic collisional processes.

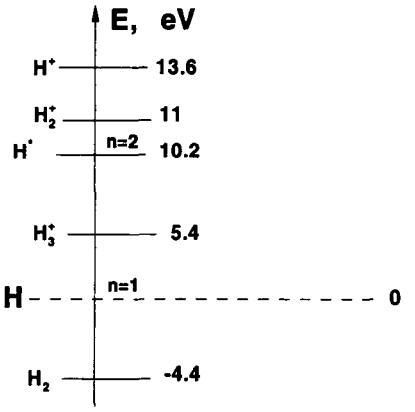

Figure 17 – Energy levels of H-species

Inelastic and elastic collisions. We include the most important inelastic process caused by electron impact (electron mobility is highest). The energy structure of the hydrogen species as adopted to enforce conservation in present model is presented in Fig.17.

Hydrogen molecule dissociation (requires 4.4eV) by electron impact (rate DH2)

$$H_2 + e \longrightarrow H + H + e \qquad (12)$$

<IDH2> = <8.5,11.7,11.7 eV> ≈ 10eV. We assume the electron loses 10eV and each H atom carries away H_2 /2 + 1/2EDH2(=(10-4.4) = 5.6eV)

Hydrogen molecule ionization by electron impact (rate IH2)

$$H_2 + e \longrightarrow e + H_2^+ + e \qquad (13)$$

Electron loses IH2= 15.4 eV, secondary electron is created with 0eV energy, H_2^+ carries away all H_2 energy.

Molecular hydrogen ion dissociation (takes 2.6eV) by electron impact (rate DH2+)

$$H_2^+ + e \longrightarrow e + H^+ + H \qquad (14)$$

{From averaged vibrational states I=2.4 eV, atom and atomic ion carry away extra <E>=4.3eV a piece in theory}. We assume electron loses IDH2+=11.2eV, and that atom and ion carry away H_2/2 + 1/2EDH2+(=8.6eV) apiece.

Hydrogen atom ionization by electron impact (rate IH)

$$H + e \longrightarrow e + H^+ + e \qquad (15)$$

Electron loses IH = 13.6eV, secondary electron at 0eV. H^+ carries H energy.

Hydrogen atom excitation by electron impact (rate EH)

$$H + e \longrightarrow e + H^*(n=2) \longrightarrow e + H + \gamma \qquad (16)$$

Electron loses IEH = 10.2eV, energy ZEH (=10.2 eV) radiated as Lyman-α.

Heavy ion formation (the only non-electron reaction, rate FH3)

$$H_2^+ + H_2 \longrightarrow H_3^+ + H \qquad (17)$$

Exothermic reaction with EFH3 = 1.2eV, evenly divided between products.

We can add the following comment on the included plasma processes. If plasma temperature is low at about 1eV then negative ions H- and vibrational-rotational levels dynamics of H_2(v,j), H2+(v,j) may be important. Other excited levels of H (n=3,4,..) may be important if plasma density goes up. Among other elementary processes to be of importance: resonance charge-

exchange H_2-H_2^+ and H-H^+, 3-body and photo recombination, Coulomb collisions, inter- and intra- elastic collisions between neutral particles and ions. Another interesting possibility is H_3^+ ion formation, but this is non-electron reaction. As plasma density is low ~$10^{12}cm^{-3}$ and temperature is moderate Te~6eV, we think that 5 mentioned reactions will be dominating.

Set of balance equations

We now can derive equations for plasma and gas density and temperature. Analysis shows that instead of temperature it's better to introduce energy density q=CnT. In this case relative equations are simpler and explicitly express energy conservation (while density equation preserves mass). By looking on reaction rates [9-10] (Fig.18) and product energies, we can draw the following conclusions:

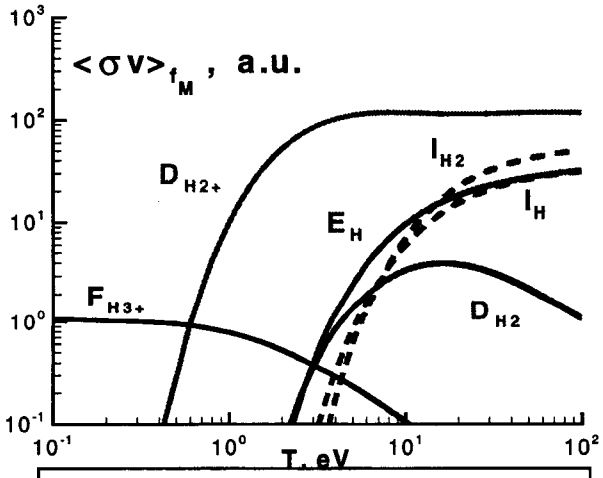

Figure 18 – Reaction rates of H-species

1) There will be a large population of Frank-Condon neutrals (via both dissociation reactions). These neutrals will be effectively transporting heat to the wall because they are not magnetized and because tube radius is much smaller than its length. Exhaust velocity of such hot neutrals will be significantly higher than that of the cold neutrals. We'd like to simulate hot component more accurately. Therefore, we split atomic neutrals into two populations – cold, H_c, with temperature $T \ll 1eV$ and hot, H_h, with $T \geq 1$-3eV.

2) Hydrogen atom excitation is more probable than ionization. So, a significant fraction of energy can be radiated as Lyman-α. Plasma is optically thin, and all radiated power will be absorbed by internal elements (antenna, etc.). Molecular ionization has slightly higher cross-section and also energy threshold if compared to atomic hydrogen. This tells that there might be a significant fraction of H_2^+ ions (and possibly H_3^+) in the discharge, depending on the H/H_2 ratio.

The system of equations has to be normalized by choosing an appropriate set of dimensionless units (typical length is 1m and thermal velocity of 1eV atom). The following units are adopted: $[n]=10^{13}cm^{-3}$, $[\sigma]=10^{-16}cm^2$, $[T]=[E]=1eV$, $[L]=1m$, $[m]=M_p$ (proton mass). We may find other units to be $[V]=(2eVk/M)^{1/2}$, $[t]=[L]/[V]\approx 0.7ms$, $[W]=[T]/[t]$, $[R]=1/[n][t]$, etc.

Equation for cold molecule density includes gas puff, molecular dissociation and excitation, particle exhaust. Equation for energy density contains related energy sinks/sources and also energy conversion at the inner wall. We presented only expression for ionization rate. The rest are obtained in a similar way. We keep calculated rates in a tabulated form to eliminate need for

their re-calculation during simulation. In these units the final form of the equations for H_{2c} mass and energy density are:

$$\frac{dn_{H2c}}{dt} = \frac{\mu}{\sigma L} - D_{H2} n_e n_{H2c} - I_{H2} n_e n_{H2c} +$$
$$F_{H3} n_{H2+} n_{H2c} - \gamma^A_{H2c} n_{H2c} V_T^{H2c}$$
$$\gamma^A_{H2c} = \frac{1}{L}$$
$$I_{H2}(T_e) = \frac{0.1}{n_e} \cdot \int_0^\infty 4\pi v^3 \sigma_{IH2} f^e_M(n_e, T_e) dv$$
$$\frac{dQ_{H2c}}{dt} = \frac{\mu}{\sigma L} Q_{H2} T^0_{H2}$$
$$-(D_{H2} n_e + I_{H2} n_e + F_{H3} n_{H2+}) Q_{H2c}$$
$$-\delta^A_{H2c} Q_{H2c} V_T^{H2c} + \delta^B_{H2c} T^W n_{H2h} V_T^{H2h}$$
$$\delta^A_{H2c} = \frac{(S+\sigma)}{\sigma L} \cdot (\alpha + \frac{C_{H2h} - 1.5}{4}) + \frac{1}{L} \cdot (C_{H2h} + 1)$$
$$\delta^B_{H2c} = \frac{C_{H2c}(S+\sigma)}{4\sigma L}, \quad C_{H2c} = \frac{5}{2}$$
$$T_{H2c} = Q_{H2c} / C_{H2c} n_{H2c}$$
$$V_T^{H2c} = \sqrt{T_{H2c}/2} \qquad (18)$$

The equations for the rest 6 plasma components can be easily obtained using similar approach. In the final dimensionless form they read are as follows. For molecular ions:

$$\frac{dn_{H2+}}{dt} = I_{H2} n_e n_{H2c} - D_{H2+} n_{H2+} n_e$$
$$- F_{H3} n_{H2+} n_{H2} - \gamma_{H2+} n_{H2+} C_S^{H2+}$$
$$\gamma_{H2+} = \frac{1}{L}$$
$$\frac{dQ_{H2+}}{dt} = I_{H2} n_e Q_{H2c} \qquad (22)$$
$$-(D_{H2+} n_e + F_{H3} n_{H2}) Q_{H2+} \qquad (19)$$
$$-\delta^A_{H2+} n_{H2+} T_{H2+} C_S^{H2+} - \delta^B_{H2+} n_{H2+} T_e C_S^{H2+}$$
$$\delta^A_{H2+} = \frac{C_{H2+}}{L}, \quad \delta^B_{H2+} = \frac{1}{L}$$
$$T_{H2+} = Q_{H2+} / C_{H2+} n_{H2+}, \quad C_{H2+} = \frac{5}{2}$$
$$V_T^{H2+} = \sqrt{T_{H2+}/2}, \quad C_S^{H2+} = \sqrt{T_e/2}$$

Equations for cold neutrals has extra particle source at the wall due to hot neutrals interacting with the wall:

$$\frac{dn_{Hc}}{dt} = -I_H n_e n_{Hc} + \gamma_{Hc}^A n_{Hh} V_T^{Hh} - \gamma_{Hc}^B n_{Hc} V_T^{Hc}$$

$$\gamma_{Hc}^A = \frac{\sigma + S}{4L\sigma}; \quad \gamma_{Hc}^B = \frac{1}{L}$$

$$\frac{dQ_{Hc}}{dt} = -I_H n_e Q_{Hc} - \delta_{Hc}^A n_{Hc} T_{Hc} V_T^{Hc} + \delta_{Hc}^B n_{Hh} T^W V_T^{Hh}$$

$$\delta_{Hc}^A = \frac{(S+\sigma)}{\sigma L} \cdot (\alpha + \frac{C_{Hc} - 1.5}{4}) + \frac{1}{L} \cdot (C_{Hc} + 1) \qquad (20)$$

$$\delta_{Hc}^B = \frac{C_{Hc}(S+\sigma)}{4\sigma L}$$

$$V_T^{Hc} = \sqrt{T_{Hc}}$$

$$T_{Hc} = Q_{Hc} / C_{Hc} n_{Hc}, \quad C_{Hc} = \frac{3}{2}$$

Equations for hot neutral account for doubled rate of hot neutrals production during molecule dissociation and their conversion to cold neutrals at the wall.

$$\frac{dn_{Hh}}{dt} = -I_H n_e n_{Hh} + 2D_{H2} n_e n_{H2c} + F_{H3} n_{H2} n_{H2+} + D_{H2+} n_e n_{H2+} - \gamma_{Hh} n_{Hh} V_T^{Hh}$$

$$\gamma_{Hh} = \frac{S + 5\sigma}{4\sigma L}$$

$$\frac{dQ_{Hh}}{dt} = -I_H n_e Q_{Hh} + D_{H2} n_e (Q_{H2c} + n_{H2c} E_{DH2}) + 0.5 D_{H2+} n_e (Q_{H2+} + n_{H2+} E_{DH2+}) + 0.5 F_{H3} (n_{H2} Q_{H2+} + n_{H2+} Q_{H2+} + n_{H2+} n_{H2} E_{FH3}) - \delta_{Hh} Q_{Hh} V_{Hh}^T$$

$$\delta_{Hh} = \frac{(S+\sigma)}{\sigma L} \cdot (\alpha + \frac{C_{Hh} - 1.5}{4}) + \frac{1}{L} \cdot (C_{Hh} + 1)$$

$$V_T^{Hh} = \sqrt{T_{Hh}}$$

$$T_{Hh} = Q_{Hh} / C_{Hh} n_{Hh}, \quad C_{Hh} = \frac{3}{2} \qquad (21)$$

Atomic ion equations account for ionization of hot and cold atomic hydrogen, dissociation of molecular ions and ion loss through the nozzle:

$$\frac{dn_{H+}}{dt} = I_H n_e (n_{Hh} + n_{Hc}) + D_{H2+} n_e n_{H2+}$$
$$- \gamma_{H+} n_{H+} C_S^{H+}; \quad \gamma_{H+} = \frac{1}{L}$$
$$\frac{dQ_{H+}}{dt} = I_H n_e (Q_{Hh} + Q_{Hc}) +$$
$$0.5 D_{H2+} n_e (Q_{H2+} + n_{H2+} E_{DH2+})$$
$$- \delta_{H+}^A n_{H+} T_{H+} C_S^{H+} - \delta_{H+}^B n_{H+} T_e C_S^{H+}$$
$$\delta_{H+}^A = \frac{1}{L} \cdot C_{H+}, \quad \delta_{H+}^B = \frac{1}{L}$$
$$V_T^{H+} = \sqrt{T_{H+}}, \quad C_S^{H+} = \sqrt{T_e}$$
$$T_{H+} = Q_{H+} / C_{H+} n_{H+}, \quad C_{H+} = \frac{3}{2} \qquad (22)$$

Heavy ion equations balance H_3^+ ion production and their exhaust into the nozzle:

$$\frac{dn_{H3}}{dt} = F_{H3} n_{H2} n_{H2+} - \gamma_{H3} n_{H3} C_S^{H3}$$
$$\gamma_{H3} = \frac{1}{L}$$
$$\frac{dQ_{H3}}{dt} = 0.5 F_{H3} (n_{H2} Q_{H2+} +$$
$$n_{H2+} Q_{H2} + n_{H2+} n_{H2} E_{F3})$$
$$- \delta_{H3}^A n_{H3} T_{H3} C_S^{H3} - \delta_{H3}^B n_{H3} T_e C_S^{H3}$$
$$\delta_{H3}^A = \frac{1}{L} \cdot C_{H3}, \quad \delta_{H3}^B = \frac{1}{L}$$
$$V_T^{H3} = \sqrt{T_{H3}/3}, \quad C_S^{H3} = \sqrt{T_e/3}$$
$$T_{H3} = Q_{H3} / C_{H3} n_{H3}, \quad C_{H3} = 2 \qquad (23)$$

Finally, the density equation for electron, because of the quasineutrality constraint, reduces to a simple form.

At the same moment energy density equation is the most elaborate. It accounts for all inelastic processes included into plasma chemistry kinetic, electron heating and electron energy carried by ion sub-sonic flow.

$$n_e = n_{H+} + n_{H2+} + n_{H3+}$$

$$\frac{dQ_e}{dt} = \frac{W}{\sigma L} - n_e I_{DH2} D_{H2c} n_{H2c}$$

$$- n_e I_{IH2} I_{H2c} n_{H2c}$$

$$- n_e I_{DH2+} D_{H2+} n_{H2+}$$

$$- n_e I_{IH} (I_{Hh} n_{Hh} + I_{Hc} n_{Hc}) \qquad (24)$$

$$- n_e I_{EH} (E_{Hh} n_{Hh} + E_{Hc} n_{Hc})$$

$$- \delta_e T_e (n_{H+} C_S^{H+} + n_{H2+} C_S^{H2+} + n_{H3} C_S^{H3})$$

$$\delta_e = \frac{1}{L} \cdot C_e, \quad C_e = \frac{3}{2}$$

$$T_e = Q_e / C_e n_e$$

For monatomic particles we used following values of specific heat coefficients: C=1.5, for diatomic species C=2.5, and for heavy ions C=3.

Benchmarking against analytical results. For relaxation oscillations see ref. [20].

Benchmarking against VX-3 experimental data.

We performed runs for the following fixed parameters of the helicon deuterium discharge: R=5cm, L=70cm, T_W=0.05eV, T_0=0.03eV. We have varied input power about W=1-2.5kW and mass of puffed gas, μ=50-130sccm. We tried to be close to experimental data: Te=5-7eV, n=1-2x10^{12}cm^{-3}. Best agreement was achieved under the following assumptions [16]:

(a) mean gas flow in the source is sub-sonic at M=0.03;
(b) plasma "parallel" flow velocity VZ=0.3Cs;
(c) electrons absorb 40% of input power.

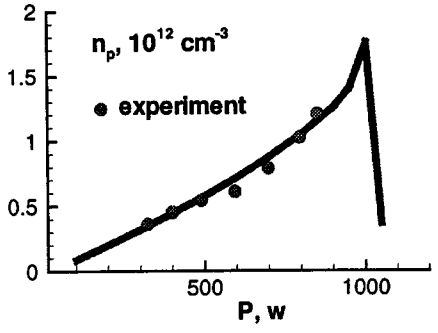

Figure 19 – density vs RF power

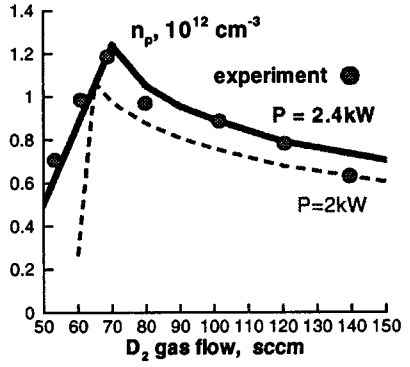

Figure 20 – density vs flow rate

In the Fig. 20 plasma density scan versus gas flow rate at fixed input power is presented. Figure 19 illustrates dependence of the plasma density versus absorbed RF-power. Agreement between simulation (solid curve) and experiment is better than 10%. Numerical model explains why plasma density goes up faster than the input power. It turns out that electron temperature goes up, making the fraction of the energy that goes into gas ionization higher with respect to radiation (Ly-α) loses.
As one can see, the 0-D mass-power balance model reproduces VX-3 experimental data quite well. The only difference is observed beyond certain input power per unit mass throughput. In the simulation we see that discharge either decays or oscillates. However, in the lab experiment this phenomenon was never observed.

Scaling VASIMR helicon operation to the MW-level power

When studying low-power VASIMR helicon plasma source we neglected radial plasma transport as unimportant. However, at higher power densities we no longer can neglect the rising radial loses to the walls. There are two major acceptable models for the cross-field transport – classical collisional and anomalous Bohm-like transport:

$$K_\perp / K_{//} \approx \frac{1.5}{\omega_{ce}^2 \tau_e^2} \approx 4\times10^{-26}\left(\frac{n_p \Lambda}{T_e^{1.5} B}\right)^2 \approx 1.5\times10^{-8} \tag{25}$$

where

$$K_\perp \approx 4.7 \frac{n_p k T_e}{m_e \omega_{ce}^2 \tau_e} \approx \frac{1.5}{\omega_{ce}^2 \tau_e^2} K_{//} \tag{26}$$

and

$$D_B \approx 0.06 \frac{ckT_e}{eB} \approx 3.2\times10^4 cm^2/\sec \tag{27}$$

The corresponding heat fluxes are given by expressions:

$$q_W \approx S\, K_\perp \nabla_R (kT_e) \approx S\, K_\perp \frac{kT_e}{R} \tag{28}$$

$$q_D \approx S\, kT_e D_B \nabla_R n_p \approx S\, kT_e D_B \frac{n_p}{R} \tag{29}$$

respectively.

Estimates show that for 20x100cm tube, 4x103cm-3 plasma density, 100eV temperature, and 1000G-field strength, the classical flux is negligible, while anomalous

$$q_D \approx 10^{-12} \frac{S T_e^2 n_p}{RB} \approx 250{,}000W \tag{30}$$

can't be ignored..

VASIMR helicon source operation simulations indicated possibility of an interesting transition to high-performance regime, see Fig. 9.

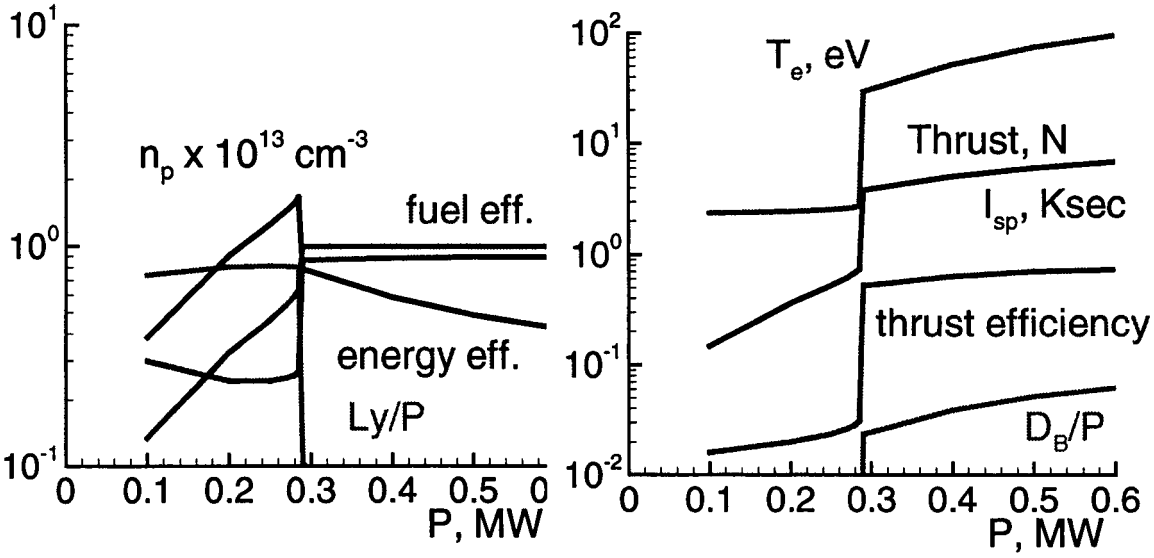

Figure 21 – High-Power scan of VASIMR discharge parameters indicating possible transition to a high-performance regime.

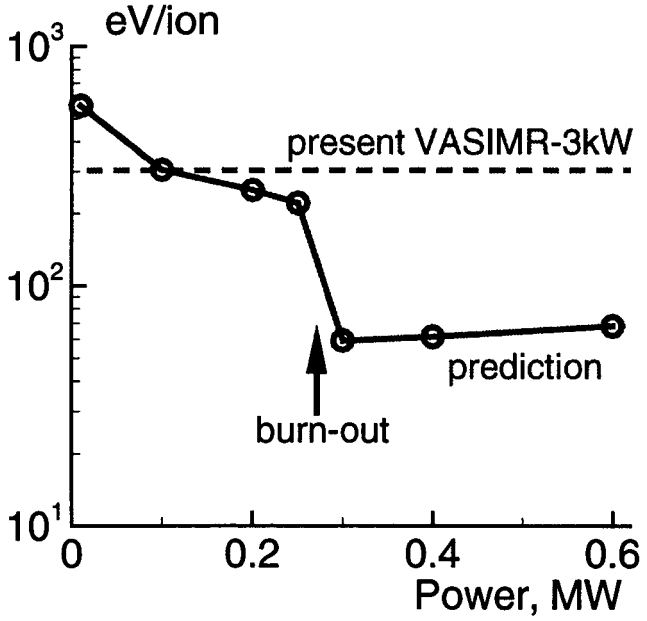

Figure 22 – Dependence of the VASIMR ionization cost versus input power. Also indicated is the presently achieved cost.

Simulations also indicate low, on the order of 60eV ionization cost for such propellant burnout regime, as follows from Fig. 22.

Conclusions

Several models have been developed under the reported period to study propellant flow and plasma conditions in the helicon plasma source of VASIMR thrusters.

The models have been benchmarked against VX-10 experiment. Numerical results demonstrate good agreement with the lab data.

The results indicate favorable VASIMR helicon source scaling to MW-level powers. The theoretically achievable

Nomenclature

B	magnetic induction ($0 - 1$ Tesla)
e	electron charge ($1.6\ 10^{-19}$ Coulomb)
E	electric field (Volt / m)
f	distribution functions
W	heating power ($0\text{-}10^{4}$ W)
I_{sp}	specific impulse ($5000 - 10^{4}$ s)
j	particle flux ($0 - 10^{21}$ / m^2 s)
k	Boltzmann constant ($1.38\ 10^{-23}$ J / K)
kT/e	temperature ($1 - 100$ electron-Volt)
L	plasma length (1 m)
σ	cross-section(m^2)
S	quartz tube surface (m^2)
M	particle mass (proton mass: $1.67\ 10^{-27}$ kg)
μ	propellant flow rate (10^{-6} kg/s)
n	density ($0 - 10^{19}$ m^{-3})
N	density ($0 - 10^{21}$ m^{-3})
R	radius of a boundary (m)
r_L	Larmor radius ($10^{-2} - 1$ m)
t	time (s)
V	exhaust velocity (10^{4} - 10^{5} m/s)
V_T	thermal velocity (ion: $10^{4} - 10^{5}$ m / s)
Cs	sound velocity (ion: $10^{4} - 10^{5}$ m / s)
$\alpha\beta\delta\gamma$	coefficients in the equations
q	heat flux (W / m^2)
λ_D	Debye length ($10^{-4} - 1$ m)
$_{mfp}$	mean free path ($0.1\text{-}1$ m)
Q	energy density (W / m^2)

Subscripts

e	electron
i	ion
H^+	hydrogen ion
H_2^+	molecular ion
H_3^+	heavy ion
H_{2c}	cold molecule
H_c	cold atom
H_h	hot atom
p	plasma
RF	radio-frequency

Conclusions

Several models have been developed under the reported period to study propellant flow and plasma conditions in the helicon plasma source of VASIMR thrusters.

The models have been benchmarked against VX-10 experiment. Numerical results demonstrate good agreement with the lab data.

The results indicate favorable VASIMR helicon source scaling to MW-level powers. The theoretically achievable

Nomenclature

B	magnetic induction ($0 - 1$ Tesla)
e	electron charge ($1.6\ 10^{-19}$ Coulomb)
E	electric field (Volt / m)
f	distribution functions
W	heating power (0-10^4 W)
I_{sp}	specific impulse ($5000 - 10^4$ s)
j	particle flux ($0 - 10^{21}$ / m^2 s)
k	Boltzmann constant ($1.38\ 10^{-23}$ J / K)
kT/e	temperature ($1 - 100$ electron-Volt)
L	plasma length (1 m)
σ	cross-section(m^2)
S	quartz tube surface (m^2)
M	particle mass (proton mass: $1.67\ 10^{-27}$ kg)
μ	propellant flow rate (10^{-6} kg/s)
n	density ($0 - 10^{19}$ m^{-3})
N	density ($0 - 10^{21}$ m^{-3})
R	radius of a boundary (m)
r_L	Larmor radius ($10^{-2} - 1$ m)
t	time (s)
V	exhaust velocity (10^4 - 10^5 m/s)
V_T	thermal velocity (ion: $10^4 - 10^5$ m / s)
Cs	sound velocity (ion: $10^4 - 10^5$ m / s)
$\alpha\beta\delta\gamma$	coefficients in the equations
q	heat flux (W / m^2)
λ_D	Debye length ($10^{-4} - 1$ m)
$_{mfp}$	mean free path (0.1-1 m)
Q	energy density (W / m^2)

Subscripts

e	electron
i	ion
H^+	hydrogen ion
H_2^+	molecular ion
H_3^+	heavy ion
H_{2c}	cold molecule
H_c	cold atom
H_h	hot atom
p	plasma
RF	radio-frequency

References

[1] Chang Díaz F.R., "Research Status of The Variable Specific Impulse Magnetoplasma Rocket", *Proc. 39th Annual Meeting of the Division of Plasma Physics* (Pittsburgh, PA, 1997), *Bulletin of APS*, **42,** 2057, 1997.

[2] Chang Díaz, F. R., Squire, J. P., Carter, M., et al., ''Recent Progress on the VASIMR'', *Proc. 41th Annual Meeting of the Division of Plasma Physics* (Seattle, WA, 1999), *Bulletin of APS*, **44**, 99, 1999.

[3] Chang Díaz, F. R., Squire, J. P., Ilin, A. V., et al. "The Development of the VASIMR Engine", *Proceedings of International Conference on Electromagnetics in Advanced Applications (ICEAA99), Sept. 13-17, 1999*, Torino, Italy, 99-102, 1999.

[4] F.R.Chang Diaz et al., "An Overview of Current Research on the VASIMR Engine", DPP-2000, Bull. APS, vol.45 (7) 129, 2000.

[5] J.P.Squire, "Recent Experimental Results in the VX-10 Device", DPP-2000, Bull. APS, vol.45 (7) 130, 2000.

[6] Braginskii, S.I., ''Transport Processes in Plasmas'' in *Reviews Plasma Phys.*, vol.1, Consultants Bureau, NY, 205, 1965.

[7] A.V.Nedospasov and M.Z.Tokar, "Wall Plasma in Tokamaks", in Reviews of Plasma Physics, Ed. Acad. B.B.Kadomtsev, Consultants Bureau, N.Y. v.18, p.77, 1993.

[8] Chen, F.F., "Plasma Ionization by Helicon Waves", *Plasma Physics and Control Fusion*, **33**, 339-364, 1991.

[9] Janev, R.K., Langer, W.D., Evans, K., Post, D.E "Elementary Processes in Hydrogen-Helium Plasmas", *Springer-Verlag*, Berlin, 1987.

[10] "Atomic and Molecular Processes in Fusion Edge Plasmas", ed. R.K.Janev, Plenum Press, N.Y. , 1995.

[11] Batishchev O., Shoucri M., Batishcheva A., Shkarofsky I., ''Fully Kinetic Simulation of Coupled Plasma and Neutral Particles in Scrape-Off Layer Plasmas of Fusion Devices'', J. Plasma Phys. **61**, 347-364, 1999.

[12] Batishchev, O ''Kinetic Model for the Variable Isp Thruster'', *Proc. 41th Annual Meeting of the Division of Plasma Physics* (Seattle, WA, 1999), *Bulletin of APS*, **44** , 99, 1999.

[13] L.B.Loeb, "The kinetic theory of gases", Dover Publications Inc., N.Y. , 1961.

[14] Schlichting H., "Boundary-Layer Theory", 7th Edition, McGraw-Hill, Inc., 1987.

[15] S.Chapman and T.G.Cowling, "The mathematical theory of non-uniform gases", Univ. Printing House, Cambridge, 1970.

[16] O.Batishchev and K.Molvig, "Kinetic Simulation of the high Isp Plasma Thruster", JPC-36, AIAA-3754 technical paper, -11p. , 2000.

[17] O.Batishchev and K.Molvig, "Study of the Operational Regimes of the VASIMR Helicon Plasma Source", DPP-2000, Quebec City, Canada, Bull. APS, 45 (7) 130, 2000

[18] O.Batishchev and K.Molvig, "Study of Mixed Collisionality Gas Flow in the VASIMR Thruster", DFD-2000, DC, USA, Bull. APS, 45 (9) 169, 2000.

[19] J.P.Squire, Private Communication, 2001, and 4th VASIMR Workshop, Houston, March, 2001.

[20] O.Batishchev and K.Molvig, "Kinetic Model of helicon plasma source for VASIMR", ACME-39, Reno, AIAA-2001-0963 technical paper, -12p., 2001.

[21] E.Bering, Private Communication, 2001, also at ACME-39, Reno, January, 2001.

[22] O.Batishchev et al, "Kinetic Effects in Tokamak Scrape-off Layer Plasmas" *Physics of Plasmas* **4** (5), 1672, May 1997

[23] O.V.Batishchev, A.A.Batishcheva, A.S. Kholodov "Unstructured adaptive grid and grid-free methods for magnetized plasma fluid simulations", *J. Plasma Phys.* **61**, part 5, 701, 1999.

[24] O.Batishchev and Kim.Molvig, "Kinetic model for a mixed collisional rarified gas flow", In. Proc. 1St MIT Conf on CFD, Cambridge, MA, USA, June 12-15, 2001.
[25] O.Batishchev and Kim.Molvig, "Modeling of a helicon plasma source" , Proc. PPPS-2001 Conf., p.157, Las Vegas, NV, USA, June 17-21, 2001.
[26] O.Batishchev and Kim.Molvig, "Numerical study of a helicon gas discharge", Annual Meeting APS DcomP, D2.006., Cambridge, June 25-28, 2001.
[27] O.Batishchev and Kim.Molvig, "Kinetic Study of the VASIMR thruster operational regimes", AIAA technical paper AIAA-20001-3501, -14p, 2001.

Publications pertained to this proposal

1. O.Batishchev, "Kinetic Model for the Variable Isp Thruster", *Bull. APS* Vol.44, No.7, 99, 1999.
2. K.Molvig, O.V.Batishchev, "A Kinetic Model for High Specific Impulse Plasma Rocket", Proceedings of the 17 th Intl. Conference on the Numerical Simulation of Plasmas, Banff, Alberta, Canada, May 22–24, 2000, p. 180.
3. O.Batishchev, K.Molvig, "Kinetic Simulation of High Isp Plasma Thruster", 36th JPC, AIAA technical paper 2000-3754, 2000, — 11p.
4. O.Batishchev, K.Molvig, «Study of Operational Regimes of the VASIMR Helicon Plasma Source», DPP/ICPP 2000 Meeting, Quebec City, Canada, Bull. APS 45 (7) 130, 2000.
5. O.Batishchev, K.Molvig, "Study of Mixed Collisionality Gas Flow in the VASIMR Thruster", 53rd Annual Meeting of the DFD, Wasington D.C., Bull. APS 45 (9) 169, 2000
6. O.Batishchev, K.Molvig, "Kinetic Model of a Helicon Plasma Source for VASIMIR", 39th ASME, AIAA technical paper 2001-0963, — 12 p, 2001
7. O.Batishchev, K.Molvig, Kinetic model for a mixed collisional rarified gas flow, First M.I.T conference on computational fluid and solid mechanics, Cambridge, MA, June 12-15, 2001
8. O.Batishchev, K.Molvig, Modeling of a helicon plasma source, o1d1, p.157, 28th IEEE ICOPS, Las Vegas, June 17-22, 2001
9. O.Batishchev, K.Molvig, Numerical study of a helicon gas discharge, D2.006, 2001 DComP APS meeting, Cambridge, MA, June 25-28, 2001
10. O.Batishchev, K.Molvig, Kinetic models for the VASIMR thruster helicon plasma source, Bull. APS 46 (8) 61, 2001
11. O.Batishchev, K.Molvig, Numerical study of plasma production in the VASIMR thruster, IEPC-01-208 paper, -19p, 27th Int. Electrical propulsion Conf., Pasadena CA, 15-19 Oct, 2001
12. O.Batishchev, K.Molvig, Numerical study of operation of the first stage of the VASIMR thruster, AIAA 2002-0347 technical paper, -12p, 40th ASME, Reno 14-17 January, 2002.
13. Oleg Batishchev and Kim Molvig, Study of gas and Plasma Conditions in the High Isp VASIMR Thruster, IAC-02-S.P.08, -11p, 53rd Intl. Astronautical Congress, 10-19 Oct, Houston, Texas, 2002
14. Kim Molvig, Oleg Batishchev, Scaling of VASIMR thruster first stage operation, 44th APS DPP Orlando 11-15 Nov, FP1.12, Bulletin APS, Vol. 47, No.9, pp.104-105, 2002

Study of Gas Burn-Out Regime in VASIMR Helicon Plasma Source

O. Batishchev[1], K. Molvig[1], F. Chang-Diaz[2], J. Squire[2]

[1]*Massachusetts Institute of Technology, Cambridge, MA 02139, USA*
[2]*ASPL, NASA Johnson Space Center, Houston, TX 77059, USA*

P-3.37

Plasma thrusters are the future

To propell in space an engine is required

For rocket propulsion K.E.Tsiolkovskii's (1895) rocket eqation is applicable

$$\frac{m}{M} = \exp\left\{-\frac{V}{E}\right\}$$

Maximum energy efficiency: E = V

Isp	(sec)	
LEO	800	
Moon	1000	
Mars (1year)	1500	
Mars (2 months)	10000	100
H + O	450	0.5

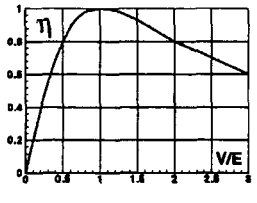

Nozzle converts T into I_{sp}

$T\,(eV) \approx (I_{sp}/10^3)^2\,\mu$

- Ideally high variable specific impulse I_{sp}=E/g is required

From Saha eq.

$n^2 = 10^{22} N T^{1.5} \exp(-E_i/T)$

for H-O n/N = 1%

! Higher I_{sp} ⇒ increased n/N = plasma

There are ~80 types of plasma thrusters

MIT

PIT Isp ~ 5 Ksec

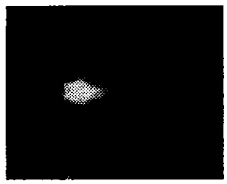

Hall effect thruster Isp ~ 4 Ksec
proposed by Morozov in 70s at KIAE

Ion thruster Isp ~ 3-10+ Ksec

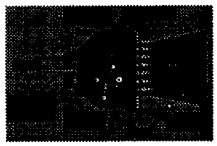

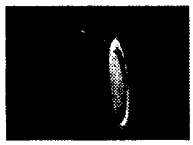

Magneto-plasma-dynamics ~ 3-10+ Ksec

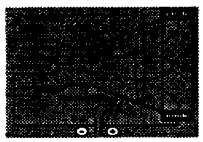

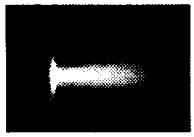

VASIMR Isp ~ 3-30+ Ksec

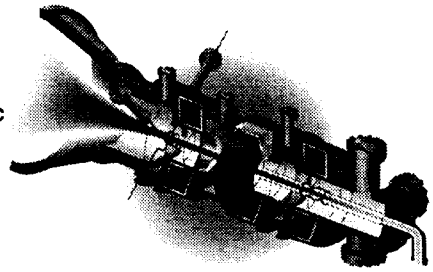

Asymmetric RF-heated double-mirror

VASIMR: Variable Specific Impulse Magnetoplasma Rocket

MIT

VASIMR was proposed at MIT ~1988
Franklin Chang-Diaz

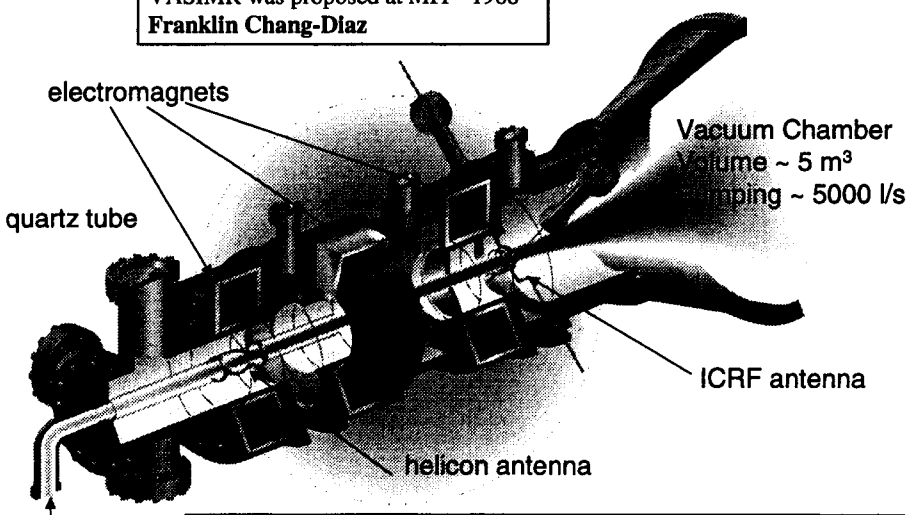

Helicon source invented in 1968 at Flinders University, South Australia
Rod Boswell

VX-10 Experiment at JSC

MIT

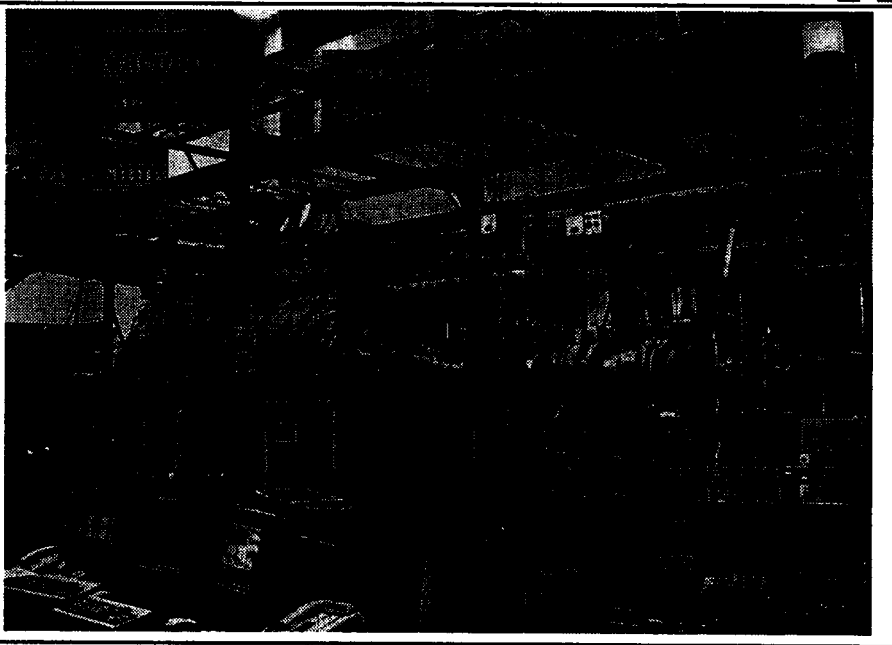

Configuration'02

MIT

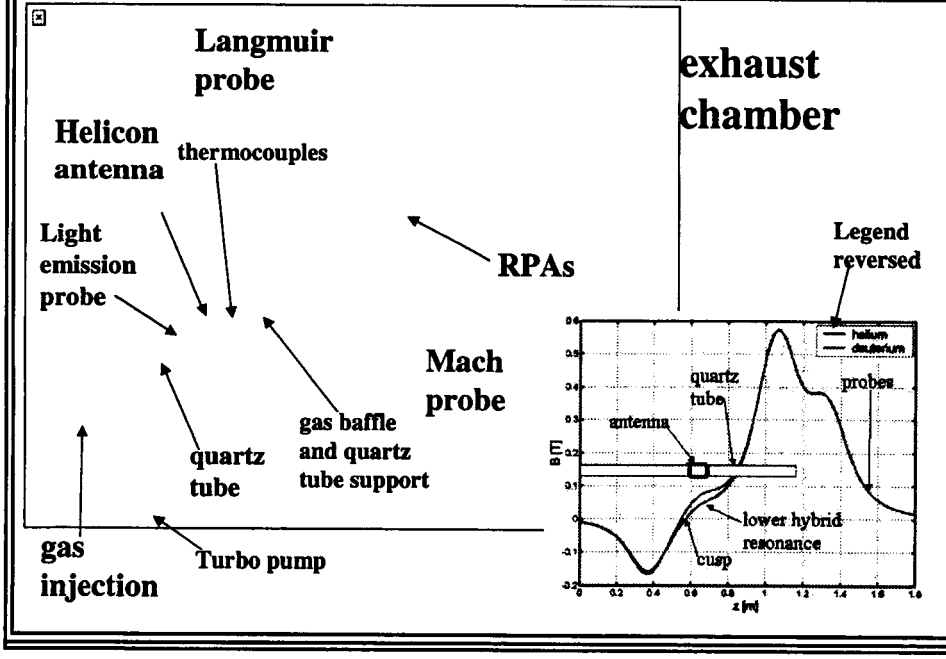

Conclusion

MIT

★ Our analysis predicted the transition of helicon source operation into the gas burnout regime, which has been observed later in the ASPL experiments

Plasma species and energy loses in H(D) and He discharge

MIT

Major ions/neutrals and energy sinks for H(D) and He propellants

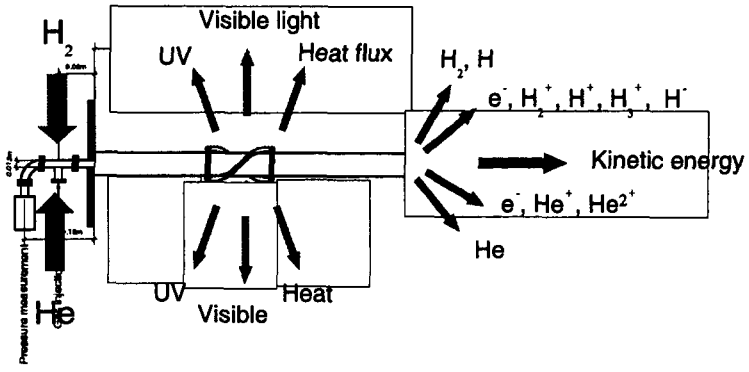

Radiation losses dominate at low $T_e \leq 4\text{-}6eV$, $\eta \approx 20\%$

Exhaust kinetic energy will dominate at higher $T_e \geq 10eV$, $\eta \approx 80\%$

Analysis of gas flow

MIT

VASIMR gas injection scheme

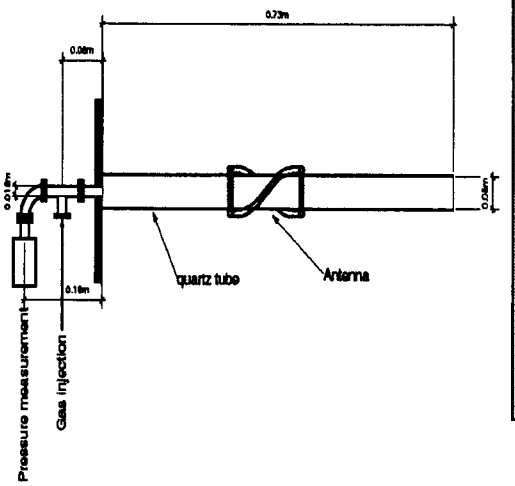

Measured (a) pressure drop P=100mtorr and (b) mass flow rate μ=80sccm gives

$R = V d / \nu \approx 20 << R_{cr} \approx 2300$

⬇

gas flow is laminar

Knudsen number

$Kn = 2\lambda/d \approx 0.1\text{-}10$

⬇

Hence, gas flow as a composition of a viscous and free molecular

1D gas flow model

MIT

Hybrid Poiseuille-Knudsen model for steady-state gas flow

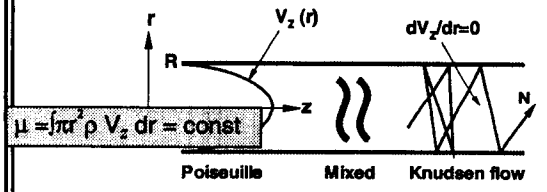

Helium gas flow inlet-quartz tube

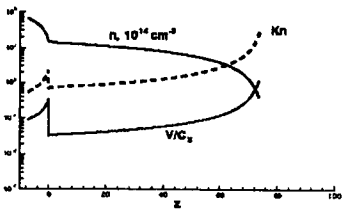

experiment ●

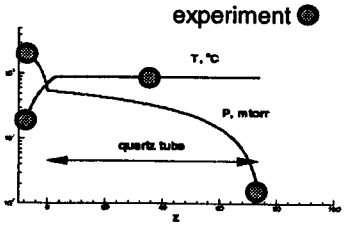

$\mu_P = a(T)\, R^4(z)\, dp/dz$

$\mu_K = b(T)\, R^3(z) dp/dz$

- $\mu = \mu_P + (\mu_K - \mu_P)\,[1 - \exp\{-K_n\}]$
  $= c(T,P,z)\, dp/dz$

$\Rightarrow$ integrate numerically equation

$\Delta p = \mu / c(T,P,z)\, \Delta z$

Kinetic study confirms viscous sub-sonic propellant flow

MIT

$$\frac{\partial f}{\partial t} + v_x \frac{\partial f}{\partial x} + v_y \frac{\partial f}{\partial y} = \frac{f_M - f}{\tau(f)} + Wall + Source$$

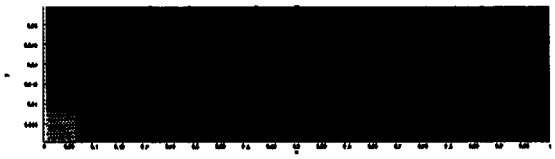

Eddy formation is possible, non-Maxwellian NDF, but overall M~0.04-0.1

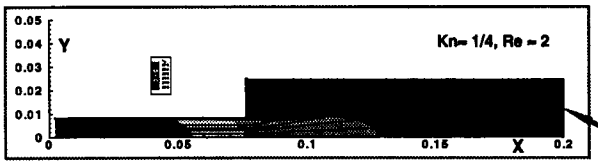

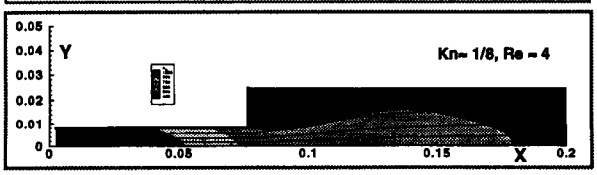

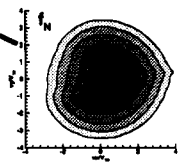

0-D model of the VASIMR plasma source (H)

MIT

Power and mass model of a helicon discharge assumes

- H_2 (D_2) at room T is puffed at a given mass flow rate μ
- a fraction of RF-power P is absorbed by electrons
- quasineutrality $\Rightarrow n_e = n_{H+} + n_{H2+} + n_{H3+}$
- plasma is magnetized, doesn't hit the wall
- hot neutrals hit wall and reflect with wall T
- gas and plasma leave the source at M≈0.1 & 1
- all 7 species {e, H_2, H_2^+, H_c, H_h, H^+, H_3^+} have Maxwellian distributions
- most important plasma-chemistry reactions are included

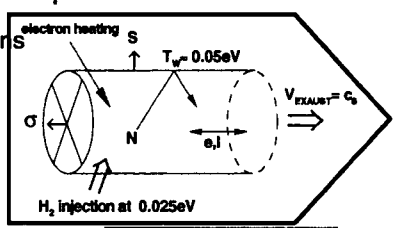

⇒ Set of 13(+1) non-linear O.D.E. with coefficients accounting for the physics and dimensions of the helicon source determines the temporal evolution of T and n of each of the plasma species

Most important plasma chemistry, H(D)

MIT

Hydrogen molecule dissociation

$$H_2 + e \rightarrow H_A + H_A + e$$

Hydrogen molecule ionization

$$H_2 + e \rightarrow e + H_2^+ + e$$

Molecular ion dissociation

$$H_2^+ + e \rightarrow H^+ + H_A + e$$

Hydrogen atom ionization

$$H + e \rightarrow e + H^+ + e$$

Hydrogen atom excitation

$$H + e \rightarrow H^* \rightarrow H + \gamma$$

Ion – neutral atom charge-exchange

$$H^+ + H \rightarrow H + H^+$$

H_3^+ ion formation

$$H_2^+ + H_2 \rightarrow H_3^+ + H_A$$

Wall conversion

$$H_A \xrightarrow{+wall} H$$

Reaction rates are sharp functions of T
⇒ analysis requires simulation

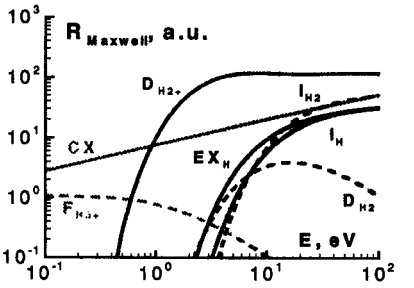

T_e has to be ≥ 6eV to reduce biggest radiative loses

$$H_2 \rightarrow H_2^+ \rightarrow H^+ + H^* \rightarrow 2H^+$$

$$H_2 \rightarrow 2H^* \rightarrow 2H^+$$

0-D balance model

MIT

Model accounts for (a) mass and energy conservation, (b) internal degrees of freedom and (c) geometry

e.g. Equations for H_2

$$\frac{dn_{H2}}{dt} = \frac{\mu}{\sigma L} - D_{H2} n_e n_{H2} - I_{H2} n_e n_{H2} - F_{H3+} n_{H2+} n_{H2} - \frac{c}{L} n_{H2} V_T^{H2}$$

$$I_{H2}(T_e) = \frac{0.1}{n_e} \cdot \int_0^{\infty} 4\pi v^3 \sigma_{IH2} f_M^e(n_e, T_e) dv$$

$$\frac{dQ_{H2}}{dt} = \frac{\mu}{\sigma L} C_{H2} T_{H2}^0 - (D_{H2} n_e + I_{H2} n_e + F_{H3+}^e n_{H2+}) Q_{H2} - \delta_{H2}^A Q_{H2} V_T^{H2} + \delta_{H2}^B T_{H2}^W n_{H2} V_T^{H2}$$

$$\delta_{H2}^A = \frac{(S+\sigma)}{\sigma L}\left(\frac{1}{\pi^{1/2}} + \frac{C_{H2}-1.5}{4}\right) + \frac{1}{L}(C_{H2}+1) \; ; \quad \delta_{H2}^B = \frac{C_{H2}(S+\sigma)}{4\sigma L}$$

$$V_T^{H2} = \sqrt{T_{H2}/2} \; ; \quad T_{H2} = Q_{H2} / C_{H2} n_{H2}$$

← H_2 if puffed, but is continuously lost for dissociation, ionization, H_3^+ formation and exhaust

← H_2 comes with room T, may acquire hot wall temperature upon collision

← Geometry and specific heat included into the conversion/exhaust coefficients

Most important plasma chemistry, He

MIT

Helium atom ionization

$$He + e \rightarrow e + He^{+} + e$$

Helium atom excitation

$$He + e \rightarrow He^{*} \rightarrow He + \gamma$$

Ion – neutral atom charge-exchange

$$He^{+} + He \rightarrow He + He^{+}$$

Helium ion ionization

$$He^{+} + e \rightarrow e + He^{2+} + e$$

Helium ion excitation

$$He^{+} + e \rightarrow He^{+*} \rightarrow He^{+} + \gamma$$

Wall conversion

$$He_{\lambda} \xrightarrow{+wall} He$$

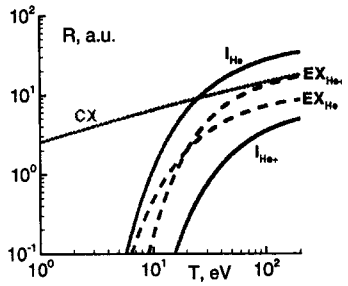

T_e has to be ≥ 6eV and ≤20eV to avoid ion radiation and double ion formation

0-D plasma kinetic model results for D_2

MIT

D_2 discharge for μ=50-130sccm flow rate and P=1-2.5kW input power has shown very good performance. Can our 0-D model reproduce it?

If (a) we take results from gas flow simulation that gas flow has M≈0.06
(b) assume that plasma "parallel" flow velocity V_z≈Cs
(c) guess that 50% of input power is absorbed by electrons
the agreement with experiment is fare

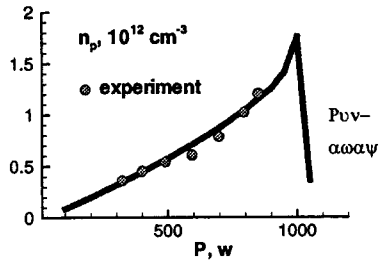

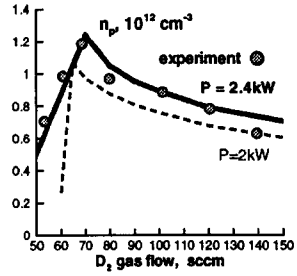

n_p vs P (μ fixed) & n_p vs μ (P fixed)

Results from 0-D model

MIT

Parameter scan for varying mass flow rate μ

- Ly-α radiation W_{rad} accounts for 25% of RF-power
- Frank-Condon neutrals W_{wall} - for 15%, which goes directly to the wall

(He forms no molecules, thus loses are less than in H(D), and easier to operate)

- The lower mass flow rate the more energy is carried out by ions W_{HI}
- Electrons carry away not more than ~3% of total input power (3kW here)

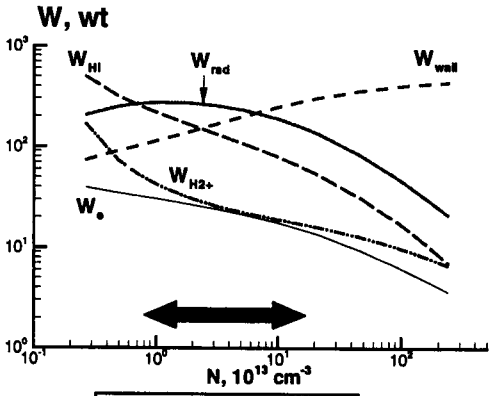

Operational regime
$N \approx 0.1\text{-}1\times10^{14}cm^{-3}$

Classical and Anomalous radial loses

MIT

Assume: $\varnothing \times L = 0.2 \times 1$ m, $n_p = 4\times10^{13}cm^{-3}$, T_e=100 eV, B=1000 G

Classical

$$K_\perp \approx 4.7\frac{n_p kT_e}{m_e\omega_{ce}^2\tau_e} \approx \frac{1.5}{\omega_{ce}^2\tau_e^2}K_{II}$$

$$K_\perp / K_{II} \approx \frac{1.5}{\omega_{ce}^2\tau_e^2} \approx 4\times10^{-26}\left(\frac{n_p\Lambda}{T_e^{1.5}B}\right)^2 \approx 1.5\times10^{-8}$$

$$q_W \approx S\,K_\perp\nabla_R(kT_e) \approx S\,K_\perp\frac{kT_e}{R}$$

$$q_W \approx 1.2\times10^{-21}S\frac{n_p^2T_e^{1/2}\Lambda}{RB^2} \approx 1{,}800W$$

Anomalous

$$D_A \approx 2\times10^4\ cm^2/\sec$$ Los Alamos Max Light

$$D_B \approx 0.06\frac{ckT_e}{eB} \approx 3.2\times10^4 cm^2/\sec$$

$$q_D \approx S\,kT_e D_B\nabla_R n_p \approx S\,kT_e D_B\frac{n_p}{R}$$

$$q_D \approx 10^{-12}\frac{ST_e^2n_p}{RB} \approx 250{,}000W$$

MW-class VASIMR helicon operation, D_2

MIT

Balance model with anomalous diffusion is applied to helicon source with following parameters

$\varnothing \times L = 0.3 \times 1$ m, μ=0.1g/sec, P~0.1-0.5 MW

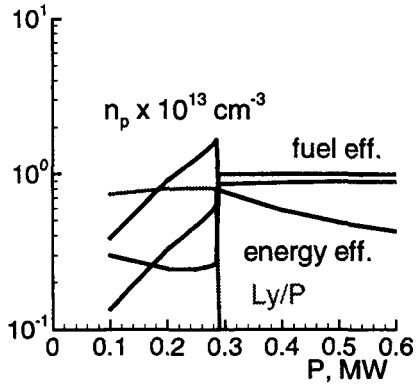

If RF coupling to plasma is high at high powers, then high source performance is achievable

⇓

- Plasma density $n_p \approx 2 \times 10^{13}$ cm^{-3}
- Propellant efficiency (cold gas to hot plasma conversion) > 90%
- Energy efficiency (gas ionization and plasma heating vs heat and radiative losses) > 80%

Single-stage VASIMR is a capable thruster

MIT

Operational regime transition occurs when most of the gas is ionized

μ=0.1g/sec = 1.5×10^{22} at/sec ⇒ 3 KW is required to heat plasma by 1eV

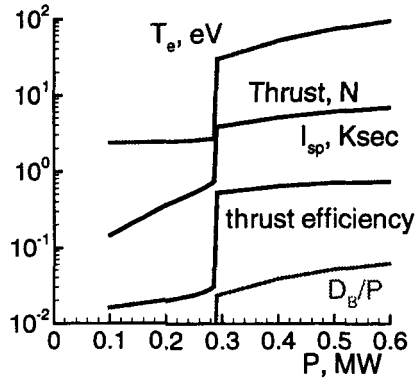

If RF coupling to plasma is high (has <u>yet to be demonstrated</u> at high P) then high thrust is achievable

⇓

- Thrust on the order of several N
- I_{sp} ~ 5-7 Ksec
- Thrust efficiency (beam energy to applied electrical energy) >50%

Ionization cost for VASIMR source

MIT

Current VASIMR-3kW helicon experiments show ~300 eV/ion production cost for H and He

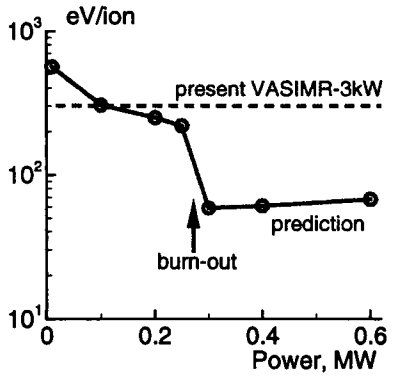

Projection: ~60 eV/ion for H

~120eV/ion for He

Other EP system costs*

Hall Effect Thruster

SPT-140 '97 – 155 eV/ion

D-100 '96 – 163

T-160 '95 – 200

P-5 '01 - 183

Ion Thruster

IAPS '83 (Hg) –258 eV/ion

NSTAR '98 (Xe) – 185

XIPS-25 '98 (Xe) – 115

Higher for MPD and PPT

J. of Propulsion and Power, vol.14, #5, 1998 and J.Haas Thesis, U.Michigan, 2001

ASPL data for D: near 100% gas utilization

MIT

- The measured ion flux scales linearly with power and gas injection rate below a saturation value
- When the gas flow is below the saturation value the electron temperature rises substantially as the flow decreases, indicating a high degree of ionization
- At the saturation values, the plasma flux equals the input neutral particle flux, within error
- Too much input gas degrades the discharge substantially

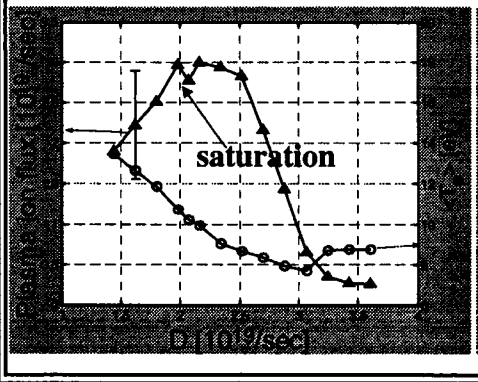

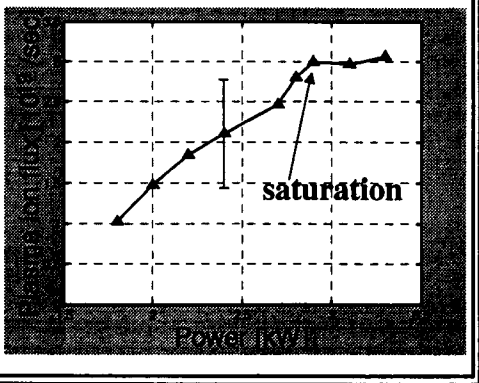

Gas burnout regime: experimental vs modeling data

MIT

Experiment

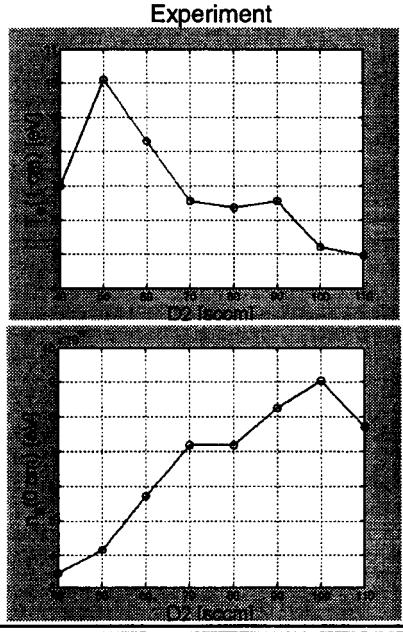

Modeling

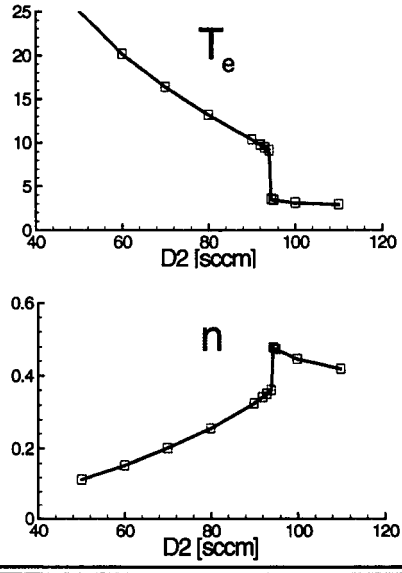

ASPL: Helium, near 100% gas utilization

MIT

Visible color change, plasma flux measurement and elevated electron temperature confirm neutral gas depletion.

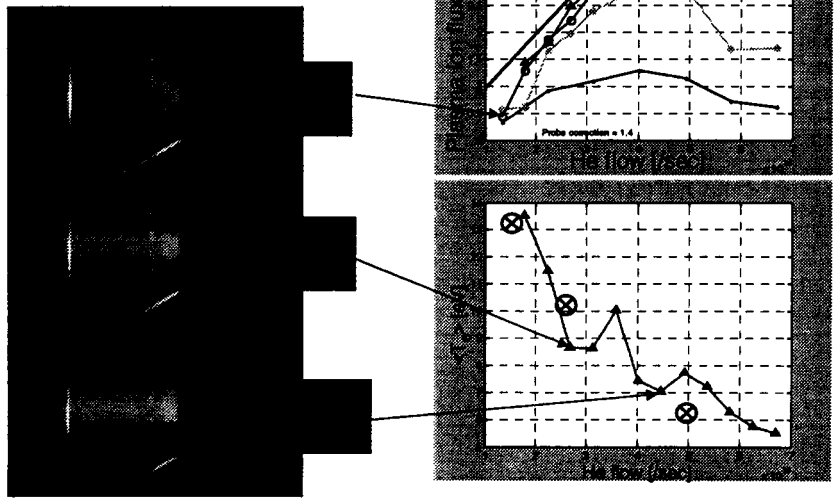

Why gas burn-out was not seen before?

MIT

- Ionization and gas utilization efficiencies are not important for plasma processing uses
- Most of the experience is with heavy gases – Ar, Kr, Xe
- Radiative loses are dominant, full ionization is impossible!

	I_1	I_2	I_3
Ar	15.8	27.6	40.7
Kr	14	24.4	37
Xe	12.1	21.2	32.1

- Energy and propellant utilization efficiencies are crucial for space applications
- Hydrogen (D) can be completely ionized. Dark plasma is feasible
- There are other interesting possibilities - Li, Cs ... H_2O, NH_3

	I_1	I_2	I_3
H	13.6		
He	24.6	54.4	
Li	5.4	76.6	122

- Gas retention by a choke, in conjunction with magnetic field mirror

Gas Choke Installed

MIT

- **The same plasma flux with half the input gas flow**
- **Higher Mach numbers measured**
- **Much lower background neutral pressures (~10^{-5} torr)**

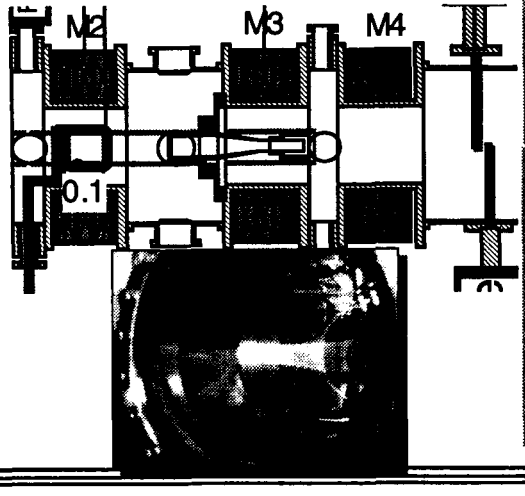

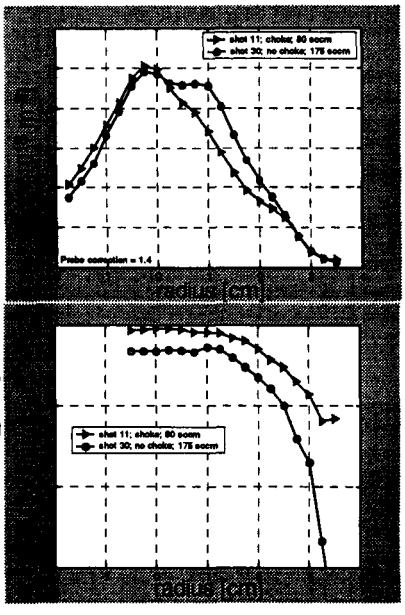

Predictive VASIMR modeling requires kinetic analysis

MIT

VX-10 experiment set-up

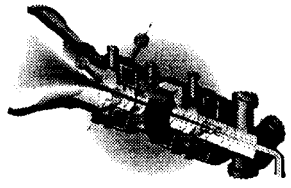

Model geometry

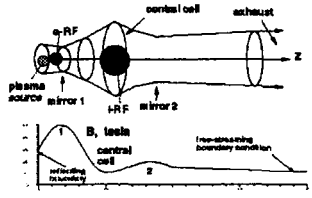

System of 2D2V kinetic equations

$$\begin{cases} \dfrac{\partial f_e}{\partial t} + v_{\parallel}\dfrac{\partial f_e}{\partial x} + \left[-D_e\dfrac{\partial^2 f_e}{\partial y^2}\right] - \dfrac{e}{m}E_{\parallel}\dfrac{\partial f_e}{\partial v_{\parallel}} + B_e = \\ \qquad C_{ee}^C + C_{ei}^C + EX_e + I_e + H_e - R_e \\ \dfrac{\partial f_i}{\partial t} + v_{\parallel}\dfrac{\partial f_i}{\partial x} + \left[-D_i\dfrac{\partial^2 f_i}{\partial y^2}\right] + \dfrac{e}{M}E_{\parallel}\dfrac{\partial f_i}{\partial v_{\parallel}} + B_i = \\ \qquad C_{ii}^C + I_i + CX_i + H_i - R_i \\ \dfrac{\partial f_N}{\partial t} + v_{\parallel}\dfrac{\partial f_N}{\partial x} + \left[v_{\perp}\dfrac{\partial f_e}{\partial y}\right] = C_{NN} - I_N + CX_N + S_N \end{cases}$$

Takes into account Coulomb, various elastic & inelsatic collisions, ambipolar and sheath potentials, mirror force, heating.

EDF and IDF in the VASIMR plasma source

MIT

1D2V kinetic model shows that the EDF is close to Maxwellian, while IDF - not

Calculated f_e and f_i

electrons

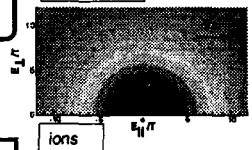

ions

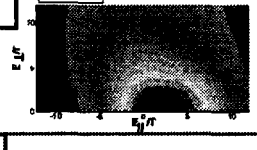

• electron heat flux, as carried by f_e, exceeds Spitzer flux by a factor of 3

• f_i is non-equilibrated due to collisions, trapping and ambipolar field

! Non-equilibrated DF's can affect diagnostics and effective reaction rates.

t = 6 Ksec

t = 4 Ksec

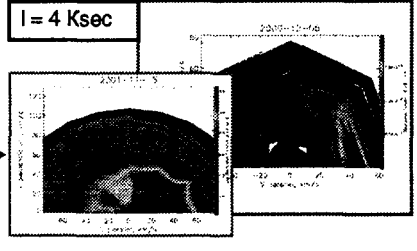

IDF as measured by RPA in VX-10 by E. Bering, 2002

Effects of ambipolar E-field and B-field trapping

MIT

RPAs show I_{sp} goes up with B-mirror ratio. Why?
T. Glover, 2001

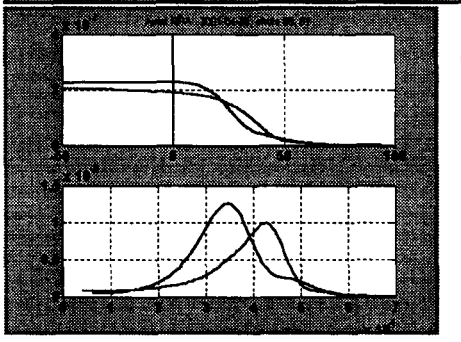

I_{sp} ≈3200s → ≈4200s

Maxwell-Boltzmann relation for a magnetic trap:

$$e\phi = T_e \ln \frac{n_{\max}}{n_{\min}}$$

For T_e≈6eV & n_{max}=2 n_{min}
ΔI_{sp} ≈1000s

Braginskii ambipolar electric field along the open magnetic lines:

$$e\phi = -1.71\nabla T_e - T_e \nabla \ln n_p$$

ϕ_Δ ≈ 30-50V → I_{sp} ≈ 4-6Ksec

! First stage of VASIMR is an effective thruster

Conclusions

MIT

★ 0-D plasma chemistry model & 1-D hybrid semi-analytical mixed collisional gas flow models are developed for the VASIMR plasma source

★ Quantitative analysis of mass/energy balance in VASIMR helicon source is done for H,D&He. Good agreement with VX-3 and VX-10 experimental data is achieved

★ 2D2V purely kinetic model for internal rarified gas flow in the system of channels is proposed and verified, shows possibility of eddy formation

★ Results from kinetic model for plasma and gas show deviation of IDF from equilibrium. Its shape is in agreement with the RPA data

★ Helicon plasma source + extended magnetic field produce ion flow with high axial drift velocity due to magnetic mirror and ambipolar potential

★ Single-stage VASIMR in the VX-10 configuration is capable of achieving I_{sp}>4Ksec & thrust ~10mN with ~50% efficiency.

★ Model has predicted transition to the gas burnout regime, which has been observed later in the ASPL experiments

★ Model predicts favorable scalability to the MW-level operation with 60eV/ion cost, >50% thrust efficiency and >7000s I_{sp}